



## Diachronous growth of the northern Tibetan plateau derived from flexural modeling

Lin Wang, Feng Cheng, Andrew Zuza, Marc Jolivet, Yiduo Liu, Zhaojie Guo,  
Xiangzhong Li, Changhao Zhang

### ► To cite this version:

Lin Wang, Feng Cheng, Andrew Zuza, Marc Jolivet, Yiduo Liu, et al.. Diachronous growth of the northern Tibetan plateau derived from flexural modeling. *Geophysical Research Letters*, 2021, 48 (8), pp.e2020GL092346. 10.1029/2020GL092346 . insu-03195723

HAL Id: insu-03195723

<https://insu.hal.science/insu-03195723>

Submitted on 7 May 2021

**HAL** is a multi-disciplinary open access archive for the deposit and dissemination of scientific research documents, whether they are published or not. The documents may come from teaching and research institutions in France or abroad, or from public or private research centers.

L'archive ouverte pluridisciplinaire **HAL**, est destinée au dépôt et à la diffusion de documents scientifiques de niveau recherche, publiés ou non, émanant des établissements d'enseignement et de recherche français ou étrangers, des laboratoires publics ou privés.

# Geophysical Research Letters

## RESEARCH LETTER

10.1029/2020GL092346

### Key Points:

- Flexural modeling shows topographic loads generated by Eastern Kunlun Shan and Qilian Shan account for the subsidence of the Qaidam basin
- We infer a low (0.4–1.0 km) Eastern Kunlun Shan and a moderate (0.4–1.5 km) Qilian Shan during the Paleogene
- Neogene surface uplift was more pronounced in the Eastern Kunlun Shan compared with Qilian Shan

### Supporting Information:

Supporting Information may be found in the online version of this article.

### Correspondence to:

F. Cheng,  
fcf.chengfeng@gmail.com

### Citation:

Wang, L., Cheng, F., Zuza, A. V., Jolivet, M., Liu, Y., Guo, Z., et al. (2021). Diachronous growth of the northern Tibetan plateau derived from flexural modeling. *Geophysical Research Letters*, 48, e2020GL092346. <https://doi.org/10.1029/2020GL092346>

Received 30 DEC 2020

Accepted 31 MAR 2021

## Diachronous Growth of the Northern Tibetan Plateau Derived From Flexural Modeling

**Lin Wang<sup>1</sup>, Feng Cheng<sup>2,3,4</sup> , Andrew V. Zuza<sup>2</sup> , Marc Jolivet<sup>5</sup> , Yiduo Liu<sup>6</sup>, Zhaojie Guo<sup>4</sup> , Xiangzhong Li<sup>7</sup>, and Changhao Zhang<sup>8</sup>**

<sup>1</sup>College of Engineering, Peking University, Beijing, China, <sup>2</sup>Nevada Bureau of Mines and Geology, University of Nevada, Reno, NV, USA, <sup>3</sup>Key Laboratory of Deep-Earth Dynamics of Ministry of Natural Resources, Institute of Geology, Chinese Academy of Geological Sciences, Beijing, China, <sup>4</sup>Key Laboratory of Orogenic Belts and Crustal Evolution, School of Earth and Space Sciences, Ministry of Education, Peking University, Beijing, China, <sup>5</sup>Géosciences Rennes–UMR CNRS 6118, Univ Rennes, Rennes, France, <sup>6</sup>Department of Earth and Atmospheric Sciences, University of Houston, TX, USA, <sup>7</sup>Yunnan Key Laboratory of Earth System Science, Yunnan University, Kunming, China, <sup>8</sup>Qinghai Oilfield Company, PetroChina, Dunhuang, Gansu, China

**Abstract** The early Cenozoic topography of the northern Tibetan plateau remains enigmatic because of the paucity of independent paleoelevation constraints. Long-held views of northward propagating deformation imply a low Paleogene elevation, but this prediction is speculative. We apply flexural modeling to reconstructed Paleogene isopach data obtained from the Qaidam basin, which requires a larger topographic load in the Qilian Shan and a smaller load in the Eastern Kunlun Shan. Incorporating knowledge of proto-Paratethys marine incursions in the Paleogene Qaidam basin, we infer a topographically low (0.4–1.0 km) Eastern Kunlun Shan and a higher (0.4–1.5 km) Qilian Shan during the Paleogene. This implied paleo-relief contrasts with previous predictions and suggests more recently, Neogene surface uplift in the Eastern Kunlun Shan has been more significant than in Qilian Shan, highlighting diachronous growth of the northern Tibetan plateau. The low-moderate paleoelevation implies a warmer and more humid climate in Northern Tibet during the Paleogene.

**Plain Language Summary** The Tibetan plateau is Earth's highest and largest plateau and has a protracted growth history closely related to Cenozoic convergence between India and Asia. Resolving its paleoelevation in the early Cenozoic is instructive to understand its growth history and Asian climate changes. Although paleoaltimetry studies have provided critical constraints for the southern Tibetan plateau during Paleogene, the paleoelevation of the northern Tibet remains enigmatic. The largest basin in the plateau is the Qaidam Basin, surrounded by high elevation thrust belts. We conducted flexural modeling of early Cenozoic strata from the Qaidam basin, which suggests higher topography in the north (0.4–1.5 km) and lower topography (0.4–1.0 km) in the south. This unique topographic relief in the northern Tibetan plateau suggests that very significant surface uplift (3–4 km) occurred along the southern margin of Qaidam basin in the late Cenozoic. These results of early topographic relief in northern Tibet support hypotheses of a Paleogene warmer and more humid climate in North Tibet. This study provides a new approach that provides an independent constraint on the Paleogene paleoelevation of northern Tibet, contributing to our understanding of the growth of the Tibetan plateau and Asian paleoclimate.

## 1. Introduction

The growth and uplift of the Tibetan plateau (Figures 1a and 1b) has implications for our knowledge of continental tectonics and intracontinental deformation (Cheng et al., 2014; Clark & Royden, 2000; DeCelles et al., 2002; Law & Allen, 2020; Murphy et al., 1997; Rowley, 1996; Tapponnier et al., 2001; Wang et al., 2008; Yin & Harrison, 2000) and the evolution of the East Asian monsoon (An et al., 2001; Clift et al., 2008; Harris, 2006; Licht et al., 2014; Molnar et al., 1993; Porter, 2001). Despite ongoing debate, numerous paleoaltimetry studies based on stable isotope hydrology, clumped isotope thermometry, and physiognomy of plant fossils have provided constraints on the early Cenozoic paleoelevation for the southern Tibetan plateau (Botsyun et al., 2019; Ding et al., 2014; Garzione et al., 2000; Hoke et al., 2014; Quade et al., 2011; Su et al., 2020). However, the early Cenozoic paleoelevation of the northern Tibetan plateau remains unclear,

© 2021. The Authors.

This is an open access article under the terms of the Creative Commons Attribution-NonCommercial License, which permits use, distribution and reproduction in any medium, provided the original work is properly cited and is not used for commercial purposes.

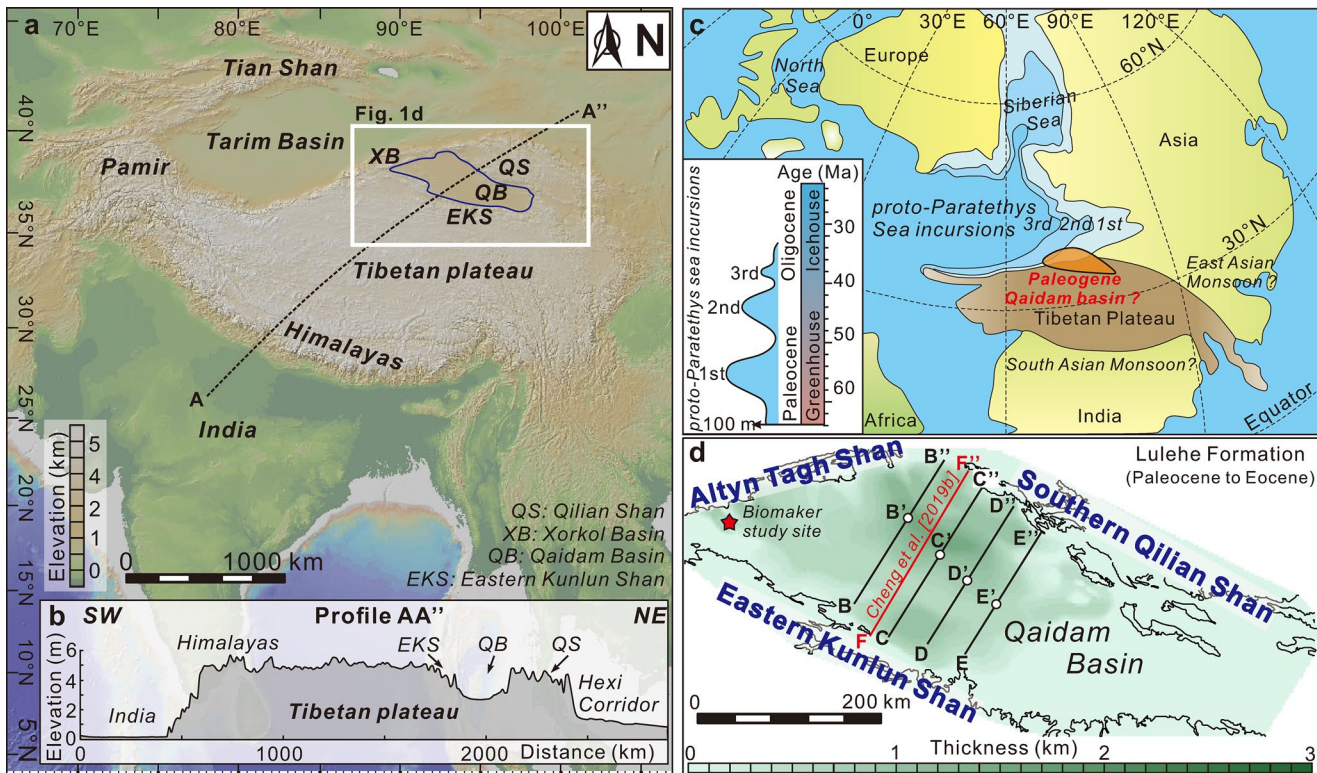


**Figure 1.** (a) Topographic map of East Asia. (b) Topographic profile AA' across the Tibetan plateau. (c) Preliminary paleogeographical map showing the incursions of the proto-Paratethys Sea, from Kaya et al. (2019). (d) Isopach map of the Paleogene Lulehe Fm. in the Qaidam basin. Red star is to the site of biomarker record reported by Ma et al. (2019).

partly due to the inapplicability of these paleoaltimetry approaches to northern Tibet (Quade et al., 2011; Rowley & Garzione, 2007; Song et al., 2020). For instance, isotope-based paleoaltimetry methods widely applied in southern Tibet cannot be used in the northern Tibetan plateau due to uncertainty between elevation and the  $\delta^{18}\text{O}$  values of meteoric waters. Due to the lack of preservation of early Cenozoic strata, physiognomy of plant fossils is also not well applied to the northern Tibetan plateau.

Currently, many studies presume negligible topography in northern Tibet during the Paleogene, mainly based on the models of northward propagating deformation across the plateau since the early Cenozoic (England & Houseman, 1986; Mulch & Chamberlain, 2006; Tapponnier et al., 2001; Wang et al., 2008) and the abundant evidence of Neogene-dominated exhumation in the northern Tibetan plateau (Duvall et al., 2013; Meyer et al., 1998; Yuan et al., 2013). In particular, it is usually assumed that the Eastern Kunlun Shan to the south was higher than the Qilian Shan during the Paleogene (Tapponnier et al., 2001; Wang et al., 2008; Wang et al., 2017). Some studies have indicated, however, that pre-Cenozoic topography might have existed in Northern Tibet, suggesting that the Paleogene paleoelevation of the northern Tibetan plateau could be partly inherited from pre-existing topographic relief (Cheng, Fu, et al., 2016; Cheng, C. N. Garzione, Jolivet, et al., 2019; Cheng, Jolivet, et al., 2019; Jolivet et al., 2001; Robinson et al., 2003). All these deductions are based on the indirect knowledge of the deformation history of the mountain belts and source to sink analysis. Paleotopography of the Tibetan plateau is also considered as an important factor that controlled the establishment of the Asian monsoon by changing the atmospheric circulation (Clift et al., 2008; Licht et al., 2014; Molnar et al., 1993; Xie et al., 2019), although there is growing appreciation for monsoon intensification driven by atmospheric  $\text{CO}_2$  concentrations and other factors (Nie et al., 2018; Ren et al., 2020). Therefore, there is an urgent need for independent paleoelevation proxies for the northern Tibetan plateau.

Recent biomarker studies indicate episodic proto-Paratethys marine incursions within the Qaidam basin, the largest depression in the Tibetan plateau (Figure 1c), since the Paleogene (Kaya et al., 2019; Ma et al., 2019).

If the Qaidam basin was at or near sea level in the early Cenozoic, a better understanding of the topographic relief of the surrounding mountain belts relative to the Qaidam basin would allow estimation of the paleoelevation of the northern Tibetan plateau. Flexural modeling provides insight into how topographic loads/relief have varied to define flexural basin geometry (P DeCelles, 2011; Royden & Karner, 1984; Saylor et al., 2018; Wang et al., 2015; Y Yang and Liu, 2002). To characterize the spatial distribution of paleorelief in the Eastern Kunlun Shan and Qilian Shan, we performed flexural modeling of four NE-trending stratigraphic sections across the Qaidam basin to reveal the lateral distribution of topographic loads/relief along the Eastern Kunlun Shan and Qilian Shan (Figure 1c). By incorporating flexural modeling results with the knowledge of proto-Paratethys marine incursion in Central Asia during the Paleogene, we further discuss the paleoelevation of northern Tibet and explore the deformation patterns of the northern Tibetan plateau.

## 2. Geological Setting

The topographically high Eastern Kunlun Shan and Qilian Shan and relatively lower Qaidam basin are the most dominant Cenozoic tectono-geomorphological features in the northern Tibetan plateau (Figures 1a and 1b). Field mapping and petroleum exploration indicate that the Qaidam basin contains as thick as >14 km of Cenozoic clastic sedimentary fill (Cheng et al., 2018; Xia et al., 2001; Yin, Dang, Wang, et al., 2008; Yin, Dang, Zhang, et al., 2008). Marking the onset of the Cenozoic sedimentation in the Qaidam basin, the Lulehe Formation (Fm.) is generally considered to be Paleocene to early Eocene in age (Chang et al., 2015; Ji et al., 2017; Ke et al., 2013; Wang et al., 2007; Yang et al., 1992; Yin, Dang, Wang, et al., 2008; W Zhang, 2007). However, recent magnetostratigraphy studies of the Lulehe Fm. at one section site in the northern Qaidam basin assigned an Oligocene or early Miocene depositional age (Figure S1) (Nie et al., 2019; W Wang et al., 2017). Given that our flexural modeling experiment is based on the entire basin-wide stratigraphic framework of the Lulehe Fm., we adopt the old age model validated by independent studies across the basin (Ji et al., 2017; Wu et al., 2019; Yin, Dang, Zhang, et al., 2008). Further discussion of the Lulehe Fm. age models is in the Supporting Information Text S1.

## 3. Approach and Method

The goal of modeling was to test for the optimal height of the Eastern Kunlun Shan and Qilian Shan that provided the best fit to the original shape of the Qaidam basin, quantified as the smallest least squares and highest coefficient of determination. To start with the modern shape of the Qaidam basin, we selected four NE-trending stratigraphic sections across the basin according to the Lulehe Fm. Isopach map obtained from the Qinghai Oilfield Company, PetroChina: Sections BB'', CC'', DD'', and EE'' (Figure 1c). We carried out shortening restoration, based on estimates of Wei et al. (2016), and sediment decompaction to obtain the original shape of the basin. Decompaction of the Lulehe Fm. strata followed the approach, porosity values, and porosity-depth coefficient of Sclater and Christie (1980). Detailed description is given in the Supporting Information Text S1 and calculation results is given in Supporting Information Data Set S1.

For an elastic infinite/continuous plate acted upon by an end load, the deflection of the lithosphere is given as (Saylor et al., 2018; Turcotte & Schubert, 2002; Wangen, 2010):

$$\omega(x) = \frac{\rho_c H W g \alpha^3}{8D} e^{-\frac{x}{\alpha}} \left( \cos \frac{x}{\alpha} + \sin \frac{x}{\alpha} \right) \quad (1)$$

where  $\omega(x)$  is the deflection at  $x$  (horizontal distance relative to the center of the load),  $\rho_c$  is the density of topographic load (crust);  $H$  and  $W$  are the height and width of the load, respectively,  $g$  is gravity,  $\alpha$  is the flexural parameter, which is a function of flexural rigidity of plate ( $D$ ), density of fluid asthenosphere ( $\rho_m$ ) and density of the basin fill ( $\rho_s$ ) and gravity ( $g$ ), given as:

$$\alpha = \left[ \frac{4D}{(\rho_m - \rho_s)g} \right]^{\frac{1}{4}} \quad (2)$$

$D$  is given as:

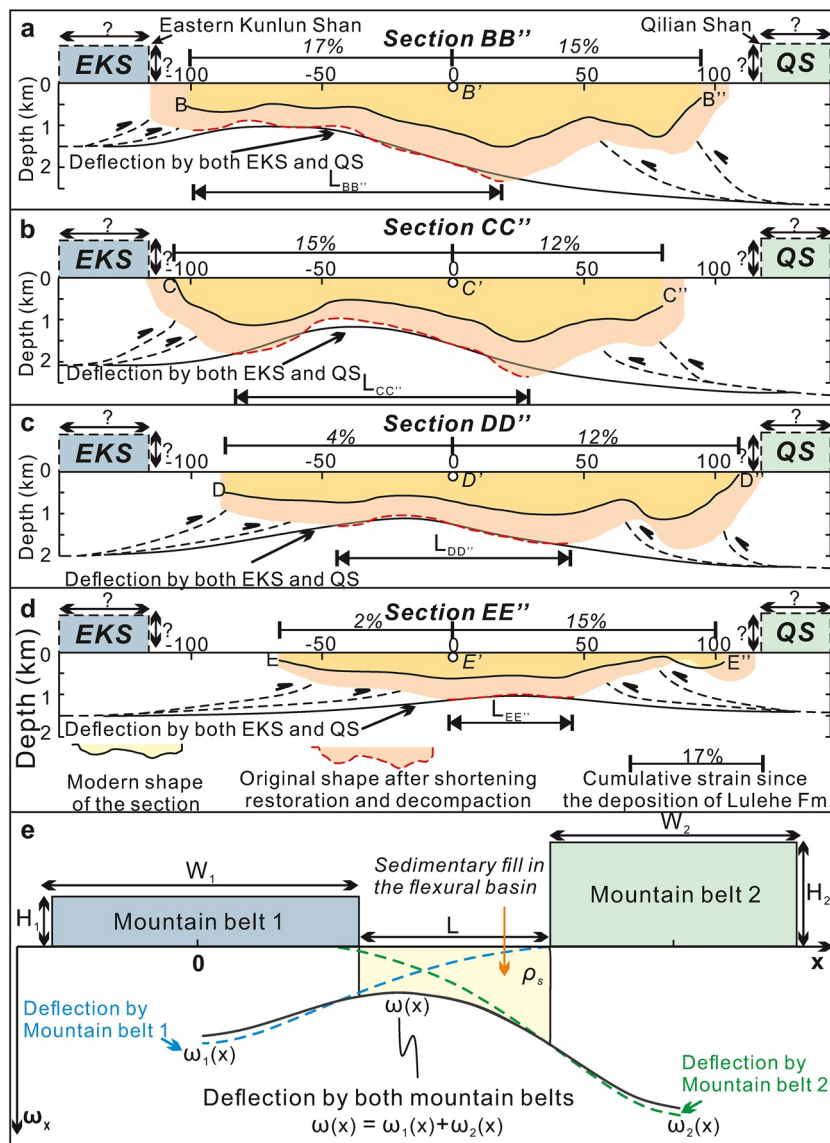


**Figure 2.** (a–d) Palinspastic section BB', CC', DD', and EE during the deposition of Lulehe Fm. after the shortening restoration and decompaction. Shortening strain is based on estimate of Wei et al. (2016). (e) Two-load beam model, showing the relationship between the topographic loads of the mountains and the deflection of the sedimentary basin. Note the modeled shape of deflection by both Eastern Kunlun Shan and Qilian Shan should match with the palinspastic shape of the associated profile. Equation for  $\omega_1(x)$  and  $\omega_2(x)$  is given in Supporting Information Text S1.

$$D = E \frac{T_e^3}{12(1 - \sigma^2)} \quad (3)$$

Flexural modeling methods of our two-load beam flexural model and uncertainty analysis are given in Figure 2e and Supporting Information Text S1. Relevant parameters (e.g., effective elastic thickness, gravity, mantel density, crustal density, basin fill density, width of the Qilian Shan and the Eastern Kunlun Shan) are in Table S1.

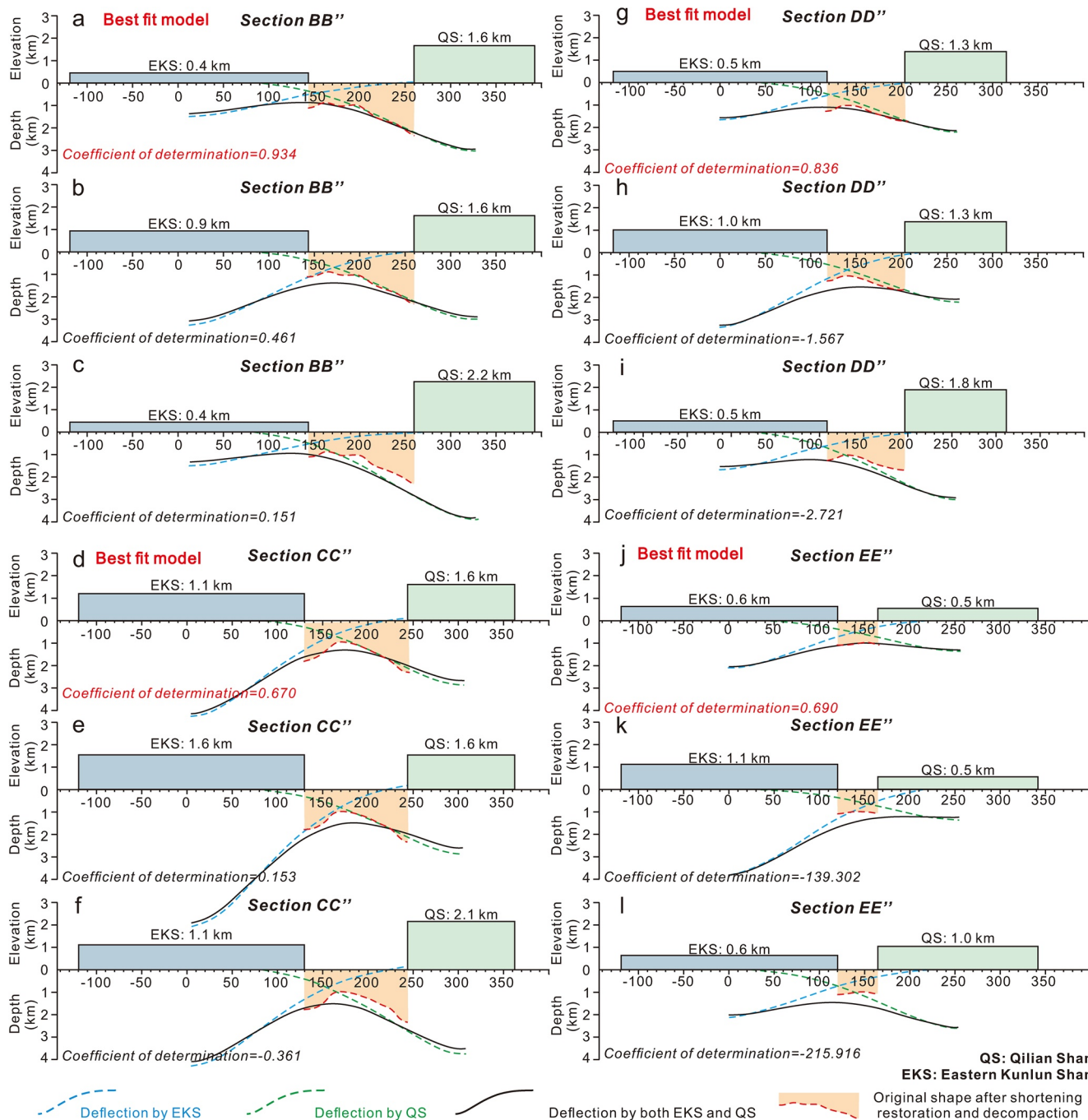


**Figure 3.** (a), (d), (g), and (j) show the modeled deflections of Qaidam basement best fits the original shape of sections BB', CC, DD, and EE', respectively. Changing parameters, for example, increasing the height of Eastern Kunlun Shan (b, e, h, k) and Qilian Shan (c, f, i, l) cannot improve the fit (a decrease in  $R^2$  value) between the modeled deflection of the Qaidam basement and the original shape of the Qaidam basin.

#### 4. Flexural Modeling and Paleoelevation Estimates

After shortening restoration and decompression, the original shapes of the sections during the deposition of the Lulehe Fm. are shown in Figure 2. Best-fit flexural modeling results, including optimal Eastern Kunlun Shan and Qilian Shan heights that recreate the shape of the Qaidam basin, are summarized in Figure 3 and Table S1. We also provide multimedia animations to show the variation of flexural modeling results when changing the effective elastic thickness and the height of the Eastern Kunlun Shan and the Qilian Shan. See

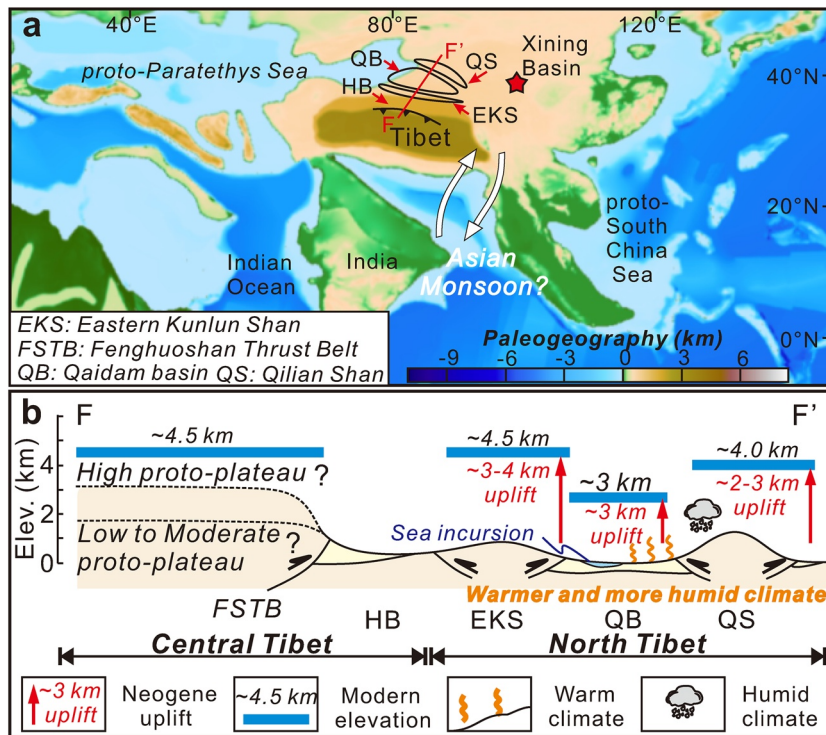


**Figure 4.** (a) Eocene (~40 Ma) paleogeographic maps of Asia showing the location of the proto-Paratethys Sea and mountain belts in Northern Tibet, modified from Poblete et al. (2021). (b) Schematic paleogeographic cross section of the central and northern Tibet, showing our proposed surface-uplift history for the northern Tibet. FSTB: Fenghuo Shan Thrust belt; EKS: Eastern Kunlun Shan; HB: Hoh Xil basin; QS: Qilian Shan; QB: Qaidam basin.

the Multimedia Animation S1-28 in the Supporting Information for more details. The code that was used to calculate the flexural modeling is given in the Supporting Information Data Set S2.

Marine incursions in the western Qaidam basin imply that it was close to proto-Paratethys sea level during the Paleogene (Kaya et al., 2019; Ma et al., 2019). With the knowledge that the proto-Paratethys sea level may have been slightly higher ( $\leq 200$  m) than global sea level (Bosboom et al., 2017; Kaya et al., 2019; Meijer et al., 2019), we then estimate that the Eastern Kunlun Shan at the southwest end of Sections B, C, D, and E was  $0.5 \pm 0.1$  km,  $1.0 \pm 0.1$  km,  $0.4 \pm 0.1$  km and  $0.5 \pm 0.1$  km high above the mean sea level (a.m.s.l.), respectively. The Qilian Shan at the northeast end of the four sections was  $1.5 \pm 0.1$  km,  $1.5 \pm 0.1$  km,  $1.2 \pm 0.1$  km, and  $0.4 \pm 0.1$  km high a.m.s.l., respectively (Table S1). The results imply that the Qilian Shan was higher in all profiles, except section E, which displays the thinnest Lulehe Fm deposits (Figure 3d) and thus may have been at the eastern extent of the Paleogene basin.

## 5. Discussion

### 5.1. Paleogene Topography of the Northern Tibetan Plateau

These flexural modeling constraints refute the existence of a negligible relief in the northern Tibetan plateau during the Paleogene (Meyer et al., 1998; Tapponnier et al., 2001), but are in agreement with independent, albeit indirect evidence suggesting Paleogene topographic relief in the northern Tibetan plateau (Figure 4a), including: 1) Eocene exhumation recorded by thermochronology (He et al., 2018; Jolivet et al., 2001; Li et al., 2020; F Wang et al., 2017); 2) proximal deposition along the margin of the Qaidam basin and Eastern Kunlun Shan/Qilian Shan provenance of Qaidam basin sediments during the Paleogene (Cheng, Guo, et al., 2015; Cheng, C. N. Garzione, Mitra, et al., 2019; Wang et al., 2020; W Wang et al., 2017; Zhang et al., 2013); and 3) Paleogene thrusts observed in seismic profiles along the Qaidam basin margin (Cheng, C. N. Garzione, Jolivet, et al., 2019; Sun et al., 2020; Wu et al., 2014; Yin et al., 2007; Yin, Dang, Zhang, et al., 2008). In particular, our flexural modeling suggests a low (0.4–1.0 km) Eastern Kunlun Shan and a

higher (0.4–1.5 km) Qilian Shan, contrasting the inference of a low Qilian Shan relative to a higher Eastern Kunlun Shan advocated by northward-propagating deformation models (England & Houseman, 1986; Tapponnier et al., 2001).

Our flexural modeling results show variable along-strike relief within the Eastern Kunlun Shan and Qilian Shan, with the Eastern Kunlun Shan showing a local topographic high in its center and the Qilian Shan yielding eastward decreasing topography. These variations may reflect lithological heterogeneities within the mountain belts or may result from their structural setting. For example, our results support a kinematic linkage between the early Cenozoic Qilian Shan and Altyn Tagh fault, resulting in higher topography closer to the Altyn Tagh fault in the west (Cheng, Jolivet, et al., 2015; Cheng, Jolivet, et al., 2016; He et al., 2018; Jolivet et al., 2001), whereas the early Cenozoic Eastern Kunlun Shan (Staisch et al., 2020) may have been an isolated thrust system with a local topographic high in its center. Variable along-strike relief in the Eastern Kunlun Shan would have developed a laterally irregular drainage divide between the Qaidam basin to the north and the Hoh Xil basin to the south. The relatively low topographic relief (~0.4 km) in the Eastern Kunlun Shan implies the possibility of drainage connection between the Qaidam and Hoh Xil basins during the Paleogene as hypothesized in the Paleo-Qaidam basin model (Cheng, Fu, et al., 2016; Cheng, C. N. Garzione, Mitra, et al., 2019; McRivette et al., 2019; Yin, Dang, Zhang, et al., 2008). On the other hand, such a potential connection should be completely cut off in those areas with a relative higher relief (~1.0 km). This finding reconciles the early Cenozoic exhumation of the Eastern Kunlun Shan (Cheng, Fu, et al., 2016; Cheng, C. N. Garzione, Mitra, et al., 2019; Wang et al., 2020; Zhang et al., 2013) with the existence of a large depression in the northern Tibet (McRivette et al., 2019; Wu, Zuza, Zhou, et al., 2019; Yin, Dang, Zhang, et al., 2008).

This unique Paleogene topographic feature in the northern Tibetan plateau indicates that the strain concentrated first in the Qilian Shan to the north, partially skipping the Eastern Kunlun Shan (Figure 4b)(Yin, Dang, Zhang, et al., 2008). Paleozoic suture zones acted as preexisting weaknesses to focus Cenozoic in both the Eastern Kunlun Shan and Qilian Shan (Allen et al., 2017; Wu et al., 2016; Zuza et al., 2016; Zuza, Wu, Wang, et al., 2018). Strength heterogeneities between the stronger North China craton and the weaker Tibetan lithosphere may have concentrated initial strain along the Qilian suture zone. After protracted crustal thickening across the Qilian Shan, it became more efficient for deformation to jump south to the Eastern Kunlun Shan. This kinematic history may have been enhanced by lithospheric buckling at a first-order wavelength of ~200 km (Bischoff & Flesch, 2018; Burg et al., 1994). Alternatively, evidence from geological mapping (Chen et al., 2012; Zuza, Wu, Reith, et al., 2018), source to sink analysis (Cheng, C. Garzione, et al., 2019; Cheng, C. N. Garzione, Mitra, et al., 2019), thermochronology (Dai et al., 2013; He et al., 2017; Jolivet et al., 2001; Liu et al., 2007), and seismic profiles (Cheng, C. Garzione, et al., 2019; Cheng, C. N. Garzione, Mitra, et al., 2019; Wu et al., 2014) suggest that the bimodal topography may reflect some pre-Cenozoic topographic inheritance in both mountain belts. However, given the unknown extent and distribution of the potential pre-existing topographic relief in the northern Tibet, it is still difficult to distinguish the contribution of pre-Cenozoic topographic inheritance from the lithospheric buckling. A more comprehensive geological investigation on the Mesozoic evolution of the northern Tibetan plateau is still needed.

Given our inferences of a low Eastern Kunlun Shan and relatively higher Qilian Shan, and considering the modern high elevation in Eastern Kunlun Shan and the Qilian Shan, we estimate ~3–4 km and ~2–3 km surface uplift after the deposition of the Lulehe Fm. in the Eastern Kunlun Shan and the Qilian Shan, respectively (Figure 4b). Cenozoic crustal shortening across the northern Tibetan plateau is sufficient to raise the elevations of the mountain ranges by these postulated magnitudes (Yin, Dang, Zhang, et al., 2008; Zuza et al., 2016). Our estimates imply that during the Neogene, substantial tectonic surface uplift concentrated more in the Eastern Kunlun Shan than in the Qilian Shan. The strength of the lithosphere and gravitational potential energy (GPE) are the two important forces that resist mountain building in the orogenic belts (Molnar & Lyon-Caen, 1988). The lithospheric strengths of the Eastern Kunlun Shan and Qilian Shan should be comparable because they share similar crustal compositions (Cheng et al., 2017; Karplus et al., 2011; Wu, Zuza, Chen, et al., 2019; Yin & Harrison, 2000; Zhao et al., 2013; Zuza, Wu, Reith, et al., 2018), which is further supported by similar elastic thickness ( $T_e$ ) estimates (Braitenberg et al., 2003).

Accordingly, GPE probably modulated the relative Neogene growth of the Qilian Shan and Eastern Kunlun Shan. As uplift-related GPE is balanced by deviatoric stress across a mountain belt, it becomes less favorable

to support continued range growth and uplift, and thus orogenic belts reach a maximum mean elevation related to the applied stress (Molnar & Lyon-Caen, 1988). Erosion of high topography with increased relief, perhaps modulated by local climate, may further drive enhanced deformation of high GPE areas (Cheng, C. N. Garzione, Mitra, et al., 2019). In northern Tibet, the present high elevation Eastern Kunlun Shan is at steady state GPE and topography whereas the Qilian Shan is at non-equilibrium state, evidenced by large maximum shear strain but negligible dilatation along the Kunlun fault and the strong negative dilatation and moderate shear strain along Haiyuan fault in the Qilian Shan derived from the GPS velocity field (M Wang & Shen, 2020). We thus infer that the Eastern Kunlun Shan reached its maximum mean elevation after the Miocene but prior to the present, due to crustal shortening and possible late Cenozoic magmatic inflation (Chen et al., 2018; Molnar et al., 1993; Yin, Dang, Zhang, et al., 2008). Since peak elevation attainment, plate convergence across the Eastern Kunlun Range has been accommodated primarily via lateral shear strain (Duvall et al., 2013; Fu & Awata, 2007; Jolivet et al., 2003; Staisch et al., 2020). Conversely, with no late Cenozoic magmatism in the Qilian Shan, Neogene convergence was partitioned in the Qilian Shan as outward growth (Bovet et al., 2009; Cheng, C. N. Garzione, Mitra, et al., 2019; Zheng et al., 2017) and/or eastward translation and block rotation (Cheng et al., 2021), preventing the Qilian Shan from reaching its maximum mean elevation.

## 5.2. Paleoclimate Implications

How and when did the Asian monsoon system develop has intrigued geoscientists for decades (An et al., 2001; Boos & Kuang, 2010; Holbourn et al., 2018; Licht et al., 2014; Nie et al., 2018; Porter, 2001; Saylor et al., 2016; Spicer, 2017; Sun & Wang, 2005; Wang et al., 2005). The well-exposed Quaternary loess-paleosol sequences and late Miocene-Pliocene red clay sequences in the Chinese Loess Plateau record the East Asian Monsoon history since the late Miocene (An et al., 1990, 2001; Ding et al., 1999; Heller & Tungsheng, 1984; Kukla, 1987; Sun et al., 1997). The finding of the dust records in the Chinese Loess Plateau and adjacent regions push the East Asian monsoon history back to late Oligocene to early Miocene (Guo et al., 2002, 2008). Recent studies further argue that a monsoon-like arid climate conditions may have initiated as early as the ~40 Ma (Licht et al., 2014, 2016) although some climate simulations challenge the establishment of a monsoon-like climate in East Asian since the Eocene (X Li et al., 2018).

Despite the importance of the atmospheric CO<sub>2</sub> concentration (Ren et al., 2020) and global cooling (Zhang et al., 2018), climate models and geological records show that the Asian paleoclimate is sensitive to the topography of the Tibetan plateau (Clift et al., 2008; Licht et al., 2014; Liu and Yin, 2002; Molnar et al., 1993; Prell & Kutzbach, 1992). The onset of the modern Asian monsoonal system has been genetically associated with the development of high topographic relief of the Tibetan-Himalayan orogen (Molnar et al., 1993), likely resulting from a Neogene rapid surface uplift of the plateau. Our inference of a low (0.4–1.0 km) Eastern Kunlun Shan and moderate (0.4–1.5 km) Qilian Shan implies a substantial Neogene surface uplift (2–4 km) of the northern Tibet which would affect the regional circulation by disrupting the general west-to-east atmospheric flow and providing a heat source that warms the atmosphere over the plateau and further strengthens its southeast flow (Molnar et al., 1993).

The lower topographic relief in the northern Tibetan plateau during the Paleogene compared with today would also allow a warmer and more humid climate with enhanced physical erosion rate and silicate weathering rates (Figure 4b). Increased erosion patterns under a warmer and wetter climate could modulate Paleogene mountain building (Cheng, C. N. Garzione, Mitra, et al., 2019; West et al., 2005) and in turn, possibly affect deformation and surface uplift (Liu et al., 2020; McQuarrie et al., 2008) in northern Tibet. Our argument of a warmer and humid climate in the northern Tibet during the Paleogene is in agreement with the magnetic susceptibility records from the Xorkol basin (J Li et al., 2018) and oxygen isotope records from the lacustrine strata in the Qaidam basin (Li and Garzione, 2017; Li et al., 2017; Mao et al., 2014; Rieser et al., 2009)(Figure S1).

## 6. Conclusions

Flexural modeling results based on Paleogene isopach data from the Qaidam basin suggest a topographic load generated by a low (0.4–1.0 km) Eastern Kunlun Shan and a moderate (0.4–1.5 km) Qilian Shan is responsible for the subsidence of the Qaidam basin during the Paleogene. We attribute the difference in paleo-reliefs in the Eastern Kunlun Shan and the Qilian Shan to the lithospheric buckling, distinctive location of the Qilian Shan against the North China, and the pre-existing topographic relief. The significant variability of the along-strike relief within the Eastern Kunlun Shan reconciles the early Cenozoic exhumation of the Eastern Kunlun Shan with the existence of a wide depression in the northern Tibet. We further propose that Neogene surface uplift in the Eastern Kunlun Shan was more significant than in the Qilian Shan. The existence of a low-to-moderate topography implies a warmer and more humid climate which in turn affected the mountain building in North Tibet. In summary, this study offers a new approach that provides an independent constraint on the Paleogene topography of North Tibet, which improves our understanding of the growth of the Tibetan plateau and Asian paleoclimate.

## Conflict of Interest

The authors declare no conflict of interest.

## Data Availability Statement

The data for the work in this paper can be downloaded from the [https://osf.io/aundx/?view\\_only=0df85d-504011448c92406a6d07ee5a72](https://osf.io/aundx/?view_only=0df85d-504011448c92406a6d07ee5a72). Supplementary figures can be found in the Supporting Information.

## Acknowledgments

Research supported by grants from the from Key Laboratory of Deep-Earth Dynamics of Ministry of Natural Resource, Institute of Geology, Chinese Academy of Geological Sciences, Beijing 100037, China (J1901), Natural Science Foundation of China (No. 41930213; 41888101; 41672163), State Key Laboratory of Loess and Quaternary Geology, Institute of Earth Environment, CAS (No. SKLLQG1903), and National Science Foundation (EAR-1914501). Insightful comments from the Editor Lucy Flesch, Kurt Sundell and an anonymous reviewer are highly appreciated.

## References

- Allen, M. B., Walters, R. J., Song, S., Saville, C., De Paola, N., Ford, J., et al. (2017). Partitioning of oblique convergence coupled to the fault locking behavior of fold-and-thrust belts: Evidence from the Qilian Shan, northeastern Tibetan Plateau. *Tectonics*, 36(9), 1679–1698. <https://doi.org/10.1002/2017tc004476>
- An, Z., John E. K., Warren L. P., & Stephen C. P. (2001). Evolution of Asian monsoons and phased uplift of the Himalaya–Tibetan plateau since Late Miocene times. *Nature*, 411(6833), 62.
- An, Z., Liu, T. S., Lu, Y., Porter, S. C., Kukla, G., Wu, X., & Hua, Y. (1990). The long-term paleomonsoon variation recorded by the loess-paleosoil sequence in Central China. *Quaternary International*, 7–8, 91–95.
- Bischoff, S. H., & Flesch, L. M. (2018). Normal faulting and viscous buckling in the Tibetan Plateau induced by a weak lower crust. *Nature Communications*, 9(1), 4952. <https://doi.org/10.1038/s41467-018-07312-9>
- Boos, W. R., & Kuang, Z. (2010). Dominant control of the South Asian monsoon by orographic insulation versus plateau heating. *Nature*, 463(7278), 218–222. <https://doi.org/10.1038/nature08707>
- Bosboom, R., Mandic, O., Dupont-Nivet, G., Proust, J.-N., Ormukov, C., & Aminov, J. (2017). Late Eocene paleogeography of the proto-Paratethys Sea in Central Asia (NW China, southern Kyrgyzstan and SW Tajikistan). *Geological Society, London, Special Publications*, 427(1), 565–588. <https://doi.org/10.1144/sp427.11>
- Botsyun, S., Sepulchre, P., Donnadieu, Y., Risi, C., Licht, A., & Caves Rugenstein, J. K. (2019). Revised paleoaltimetry data show low Tibetan Plateau elevation during the Eocene. *Science*, 363(6430), eaq1436. <https://doi.org/10.1126/science.aaq1436>
- Bovet, P. M., Ritts, B. D., Gehrels, G., Abbink, A. O., Darby, B., & Hourigan, J. (2009). Evidence of Miocene crustal shortening in the north Qilian Shan from Cenozoic stratigraphy of the western Hexi Corridor, Gansu Province, China. *American Journal of Science*, 309(4), 290–329. <https://doi.org/10.2475/00.4009.02>
- Braitenberg, C., Wang, Y., Fang, J., & Hsu, H. T. (2003). Spatial variations of flexure parameters over the Tibet–Qinghai plateau. *Earth and Planetary Science Letters*, 205(3), 211–224. [https://doi.org/10.1016/s0012-821x\(02\)01042-7](https://doi.org/10.1016/s0012-821x(02)01042-7)
- Burg, J.-P., Davy, P., & Martinod, J. (1994). Shortening of analogue models of the continental lithosphere: New hypothesis for the formation of the Tibetan plateau. *Tectonics*, 13(2), 475–483. <https://doi.org/10.1029/93tc02738>
- Chang, H., Li, L., Qiang, X., Garzione, C. N., Pullen, A., & An, Z. (2015). Magnetostratigraphy of Cenozoic deposits in the western Qaidam Basin and its implication for the surface uplift of the northeastern margin of the Tibetan Plateau. *Earth and Planetary Science Letters*, 430, 271–283. <https://doi.org/10.1016/j.epsl.2015.08.029>
- Cheng, F., Fu, S., Jolivet, M., Zhang, C., & Guo, Z. (2016a). Source to sink relation between the Eastern Kunlun Range and the Qaidam Basin, northern Tibetan Plateau, during the Cenozoic. *Geological Society of America Bulletin*, 128(1–2), 258–283.
- Cheng, F., Garzione, C., Jolivet, M., Guo, Z., Zhang, D., & Zhang, C. (2018). A new sediment accumulation model of Cenozoic depositional ages from the Qaidam Basin, Tibetan Plateau. *Journal of Geophysical Research Earth Surface*, 123(11), 3101–3121. <https://doi.org/10.1029/2018jf004645>
- Cheng, F., Garzione, C., Jolivet, M., Wang, W., Dong, J., Richter, F., & Guo, Z. (2019a). Provenance analysis of the Yumen Basin and northern Qilian Shan: Implications for the pre-collisional paleogeography in the NE Tibetan plateau and eastern termination of Altyn Tagh fault. *Gondwana Research*, 65, 156–171. <https://doi.org/10.1016/j.gr.2018.08.009>
- Cheng, F., Garzione, C. N., Jolivet, M., Guo, Z., Zhang, D., Zhang, C., & Zhang, Q. (2019b). Initial deformation of the Northern Tibetan Plateau: Insights from deposition of the Lulehe formation in the Qaidam Basin. *Tectonics*, 38, 741–766. <https://doi.org/10.1029/2018tc005214>

- Cheng, F., Garzzone, C. N., Mitra, G., Jolivet, M., Guo, Z., Lu, H., et al. (2019c). The interplay between climate and tectonics during the upward and outward growth of the Qilian Shan orogenic wedge, northern Tibetan Plateau. *Earth-Science Reviews*, 198, 102945. <https://doi.org/10.1016/j.earscirev.2019.102945>
- Cheng, F., Guo, Z., Jenkins, H. S., Fu, S., & Cheng, X. (2015a). Initial rupture and displacement on the Altyn Tagh fault, northern Tibetan Plateau: Constraints based on residual Mesozoic to Cenozoic strata in the western Qaidam Basin. *Geosphere*, 11(3), 921–942. <https://doi.org/10.1130/ges01070.1>
- Cheng, F., Jolivet, M., Dupont-Nivet, G., Wang, L., Yu, X., & Guo, Z. (2015b). Lateral extrusion along the Altyn Tagh Fault, Qilian Shan (NE Tibet): Insight from a 3D crustal budget. *Terra Nova*, 27(6), 416–425. <https://doi.org/10.1111/ter.12173>
- Cheng, F., Jolivet, M., Fu, S., Zhang, C., Zhang, Q., & Guo, Z. (2016b). Large-scale displacement along the Altyn Tagh Fault (North Tibet) since its Eocene initiation: Insight from detrital zircon U-Pb geochronology and subsurface data. *Tectonophysics*, 677–678, 261–279. <https://doi.org/10.1016/j.tecto.2016.04.023>
- Cheng, F., Jolivet, M., Fu, S., Zhang, Q., Guan, S., Yu, X., & Guo, Z. (2014). Northward growth of the Qimen Tagh Range: A new model accounting for the Late Neogene strike-slip deformation of the SW Qaidam Basin. *Tectonophysics*, 632(0), 32–47. <https://doi.org/10.1016/j.tecto.2014.05.034>
- Cheng, F., Jolivet, M., Guo, Z., Lu, H., Zhang, B., Li, X., et al. (2019d). Jurassic-Early Cenozoic tectonic inversion in the Qilian Shan and Qaidam Basin, North Tibet: New insight from seismic reflection, isopach mapping, and drill core data. *Journal of Geophysical Research Soild Earth*, 124(11), 12077–12098. <https://doi.org/10.1029/2019jb018086>
- Cheng, F., Jolivet, M., Hallot, E., Zhang, D., Zhang, C., & Guo, Z. (2017). Tectono-magmatic rejuvenation of the Qaidam craton, northern Tibet. *Gondwana Research*, 49, 248–263. <https://doi.org/10.1016/j.gr.2017.06.004>
- Cheng, F., Zupa, A. V., Hapgood, P. J., Wu, C., Neudorf, C., Chang, H., et al. (2021). Accommodation of India-Asia convergence via strike-slip faulting and block rotation in the Qilian Shan fold-thrust belt, northern margin of the Tibetan Plateau. *Journal of the Geological Society*
- Chen, J.-L., Yin, A., Xu, J.-F., Dong, Y.-H., & Kang, Z.-Q. (2018). Late Cenozoic magmatic inflation, crustal thickening, and >2 km of surface uplift in central Tibet. *Geology*, 46(1), 19–22. <https://doi.org/10.1130/g39699.1>
- Chen, X., Gehrels, G., Yin, A., Li, L., & Jiang, R. B. (2012). Paleozoic and Mesozoic basement magmatism of Eastern Qaidam Basin, Northern Qinghai-Tibet Plateau: LA-ICP-MS Zircon U-Pb geochronology and its geological significance. *Acta Geologica Sinica - English Edition*, 86(2), 350–369.
- Clark, M. K., & Royden, L. H. (2000). Topographic ooze: Building the eastern margin of Tibet by lower crustal flow. *Geology*, 28(8), 703–706. [https://doi.org/10.1130/0091-7613\(2000\)28<703:tobtem>2.0.co;2](https://doi.org/10.1130/0091-7613(2000)28<703:tobtem>2.0.co;2)
- Clift, P. D., Hodges, K. V., Heslop, D., Hannigan, R., Van Long, H., & Calves, G. (2008). Correlation of Himalayan exhumation rates and Asian monsoon intensity. *Nature Geoscience*, 1(12), 875–880. <https://doi.org/10.1038/ngeo351>
- Dai, J., Wang, C., Hourigan, J., & Santosh, M. (2013). Multi-stage tectono-magmatic events of the Eastern Kunlun Range, northern Tibet: Insights from U-Pb geochronology and (U-Th)/He thermochronology. *Tectonophysics*, 599, 97–106. <https://doi.org/10.1016/j.tecto.2013.04.005>
- DeCelles, P. (2011). Foreland basin systems revisited: Variations in response to tectonic settings. In *Tectonics of sedimentary basins. Recent advances* (pp. 405–426). Wiley-Blackwell.
- DeCelles, P. G., Robinson, D. M., & Zandt, G. (2002). Implications of shortening in the Himalayan fold-thrust belt for uplift of the Tibetan plateau. *Tectonics*, 21(6), 12–11–12–25. <https://doi.org/10.1029/2001tc001322>
- Ding, L., Xu, Q., Yue, Y., Wang, H., Cai, F., & Li, S. (2014). The Andean-type Gangdese Mountains: Paleoelevation record from the Paleocene-Eocene Linzhou Basin. *Earth and Planetary Science Letters*, 392, 250–264. <https://doi.org/10.1016/j.epsl.2014.01.045>
- Ding, Z. L., Xiong, S. F., Sun, J. M., Yang, S. L., Gu, Z. Y., & Liu, T. S. (1999). Pedostratigraphy and paleomagnetism of a ~7.0 Ma eolian loess-red clay sequence at Lingtai, Loess Plateau, north-central China and the implications for paleomonsoon evolution. *Palaeogeography, Palaeoclimatology, Palaeoecology*, 152(1), 49–66. [https://doi.org/10.1016/s0031-0182\(99\)00034-6](https://doi.org/10.1016/s0031-0182(99)00034-6)
- Duvall, A. R., Clark, M. K., Kirby, E., Farley, K. A., Craddock, W. H., Li, C., & Yuan, D.-Y. (2013). Low-temperature thermochronometry along the Kunlun and Haiyuan Faults, NE Tibetan Plateau: Evidence for kinematic change during late-stage orogenesis. *Tectonics*, 32(5), 1190–1211. <https://doi.org/10.1002/tect.20072>
- England, P., & Houseman, G. (1986). Finite strain calculations of continental deformation: 2. Comparison with the India-Asia collision zone. *Journal of Geophysical Research*, 91(B3), 3664–3676. <https://doi.org/10.1029/jb091ib03p03664>
- Fu, B., & Awata, Y. (2007). Displacement and timing of left-lateral faulting in the Kunlun fault zone, northern Tibet, inferred from geologic and geomorphic features. *Journal of Asian Earth Sciences*, 29(2), 253–265. <https://doi.org/10.1016/j.jseaes.2006.03.004>
- Garzzone, C. N., Dettman, D. L., Quade, J., DeCelles, P. G., & Butler, R. F. (2000). High times on the Tibetan Plateau: Paleoelevation of the Thakkhola graben, Nepal. *Geology*, 28(4), 339–342. [https://doi.org/10.1130/0091-7613\(2000\)028<0339:htottp>2.3.co;2](https://doi.org/10.1130/0091-7613(2000)028<0339:htottp>2.3.co;2)
- Guo, Z. T., Ruddiman, W. F., Hao, Q. Z., Wu, H. B., Qiao, Y. S., Zhu, R. X., et al. (2002). Onset of Asian desertification by 22 Myr ago inferred from loess deposits in China. *Nature*, 416(6877), 159–163. <https://doi.org/10.1038/416159a>
- Guo, Z. T., Sun, B., Zhang, Z. S., Peng, S. Z., Xiao, G. Q., Ge, J. Y., et al. (2008). A major reorganization of Asian climate by the early Miocene. *Climate of the Past*, 4(3), 153–174. <https://doi.org/10.5194/cp-4-153-2008>
- Harris, N. (2006). The elevation history of the Tibetan Plateau and its implications for the Asian monsoon. *Palaeogeography, Palaeoclimatology, Palaeoecology*, 241(1), 4–15. <https://doi.org/10.1016/j.palaeo.2006.07.009>
- He, P., Song, C., Wang, Y., Chen, L., Chang, P., Wang, Q., & Ren, B. (2017). Cenozoic exhumation in the Qilian Shan, northeastern Tibetan Plateau: Evidence from detrital fission track thermochronology in the Jiuquan Basin. *Journal of Geophysical Research Soild Earth*, 122(8), 6910–6927. <https://doi.org/10.1002/2017jb014216>
- He, P., Song, C., Wang, Y., Meng, Q., Chen, L., Yao, L., et al. (2018). Cenozoic deformation history of the Qilian Shan (northeastern Tibetan Plateau) constrained by detrital apatite fission-track thermochronology in the northeastern Qaidam Basin. *Tectonophysics*, 749, 1–11. <https://doi.org/10.1016/j.tecto.2018.10.017>
- Heller, F., & Tungsheng, L. (1984). Magnetism of Chinese loess deposits. *Geophysical Journal International*, 77(1), 125–141. <https://doi.org/10.1111/j.1365-246x.1984.tb01928.x>
- Hoke, G. D., Liu-Zeng, J., Hren, M. T., Wissink, G. K., & Garzzone, C. N. (2014). Stable isotopes reveal high southeast Tibetan Plateau margin since the Paleogene. *Earth and Planetary Science Letters*, 394, 270–278. <https://doi.org/10.1016/j.epsl.2014.03.007>
- Holbourn, A. E., Kuhnt, W., Clemens, S. C., Kochhann, K. G. D., Jöhnck, J., Lübbers, J., & Andersen, N. (2018). Late Miocene climate cooling and intensification of southeast Asian winter monsoon. *Nature Communications*, 9(1), 1584. <https://doi.org/10.1038/s41467-018-03950-1>
- Ji, J., Zhang, K., Clift, P. D., Zhuang, G., Song, B., Ke, X., & Xu, Y. (2017). High-resolution magnetostratigraphic study of the Paleogene-Neogene strata in the Northern Qaidam Basin: Implications for the growth of the Northeastern Tibetan Plateau. *Gondwana Research*, 46, 141–155. <https://doi.org/10.1016/j.gr.2017.02.015>

- Jolivet, M., Brunel, M., Seward, D., Xu, Z., Yang, J., Malavieille, J., et al. (2003). Neogene extension and volcanism in the Kunlun Fault Zone, northern Tibet: New constraints on the age of the Kunlun Fault. *Tectonics*, 22(5), 1052. <https://doi.org/10.1029/2002tc001428>
- Jolivet, M., Brunel, M., Seward, D., Xu, Z., Yang, J., Roger, F., et al. (2001). Mesozoic and Cenozoic tectonics of the northern edge of the Tibetan plateau: Fission-track constraints. *Tectonophysics*, 343(1–2), 111–134. [https://doi.org/10.1016/s0040-1951\(01\)00196-2](https://doi.org/10.1016/s0040-1951(01)00196-2)
- Karplus, M. S., Zhao, W., Klemperer, S. L., Wu, Z., Mechler, J., Shi, D., et al. (2011). Injection of Tibetan crust beneath the south Qaidam Basin: Evidence from INDEPTH IV wide-angle seismic data. *Journal of Geophysical Research*, 116(B7), B07301. <https://doi.org/10.1029/2010jb007911>
- Kaya, M. Y., Dupont-Nivet, G., Proust, J. N., Roperch, P., Bougeois, L., Meijer, N., et al. (2019). Paleogene evolution and demise of the proto-Paratethys Sea in Central Asia (Tarim and Tadjik basins): Role of intensified tectonic activity at ca. 41 Ma. *Basin Research*, 31(3), 461–486. <https://doi.org/10.1111/bre.12330>
- Ke, X., Ji, J., Zhang, K., Kou, X., Song, B., & Wang, C. (2013). Magnetostratigraphy and anisotropy of magnetic susceptibility of the lulehe formation in the Northeastern Qaidam Basin. *Acta Geologica Sinica—English Edition*, 87(2), 576–587.
- Kukla, G. (1987). Loess stratigraphy in central China. *Quaternary Science Reviews*, 6(3), 191–219. [https://doi.org/10.1016/0277-3791\(87\)90004-7](https://doi.org/10.1016/0277-3791(87)90004-7)
- Law, R., & Allen, M. B. (2020). Diachronous Tibetan Plateau landscape evolution derived from lava field geomorphology. *Geology*, 48(3), 263–267. <https://doi.org/10.1130/g47196.1>
- Li, B., Zuza, A. V., Chen, X., Hu, D., Shao, Z., Qi, B., et al. (2020). Cenozoic multi-phase deformation in the Qilian Shan and out-of-sequence development of the northern Tibetan Plateau. *Tectonophysics*, 782–783, 228423.
- Li, J., Yue, L., Roberts, A., Hirt, A. M., Pan, F., Guo, L., et al. (2018). Global cooling and enhanced Eocene Asian mid-latitude interior aridity. *Nature Communications*, 9(1), 3026. <https://doi.org/10.1038/s41467-018-05415-x>
- Li, L., & Garzione, C. N. (2017). Spatial distribution and controlling factors of stable isotopes in meteoric waters on the Tibetan Plateau: Implications for paleoelevation reconstruction. *Earth and Planetary Science Letters*, 460, 302–314. <https://doi.org/10.1016/j.epsl.2016.11.046>
- Li, L.-L., Wu, C.-D., Fan, C.-F., Li, J.-J., & Zhang, C.-H. (2017). Carbon and oxygen isotopic constraints on paleoclimate and paleoelevation of the southwestern Qaidam basin, northern Tibetan Plateau. *Geoscience Frontiers*, 8(5), 1175–1186. <https://doi.org/10.1016/j.gsf.2016.12.001>
- Li, X., Zhang, R., Zhang, Z., & Yan, Q. (2018). Do climate simulations support the existence of East Asian monsoon climate in the Late Eocene? *Palaeogeography, Palaeoclimatology, Palaeoecology*, 509, 47–57. <https://doi.org/10.1016/j.palaeo.2017.12.037>
- Licht, A., Dupont-Nivet, G., Pullen, A., Kapp, P., Abels, H., Lai, Z., et al. (2016). Resilience of the Asian atmospheric circulation shown by Paleogene dust provenance. *Nature Communications*, 7. <https://doi.org/10.1038/ncomms12390>
- Licht, A., Van Cappelle, M., Abels, H. A., Ladant, J.-B., Trabucho-Alexandre, J., France-Lanord, C., et al. (2014). Asian monsoons in a late Eocene greenhouse world. *Nature*, 513(7519), 501–506. <https://doi.org/10.1038/nature13704>
- Liu, X., & Yin, Z.-Y. (2002). Sensitivity of East Asian monsoon climate to the uplift of the Tibetan Plateau. *Palaeogeography, Palaeoclimatology, Palaeoecology*, 183(3), 223–245. [https://doi.org/10.1016/s0031-0182\(01\)00488-6](https://doi.org/10.1016/s0031-0182(01)00488-6)
- Liu, Y.-J., Neubauer, F., Gensler, J., Ge, X.-H., Takasu, A., Yuan, S.-H., et al. (2007). Geochronology of the initiation and displacement of the Altyn Strike-Slip Fault, western China. *Journal of Asian Earth Sciences*, 29(2), 243–252. <https://doi.org/10.1016/j.jseas.2006.03.002>
- Liu, Y., Tan, X., Ye, Y., Zhou, C., Lu, R., Murphy, M. A., et al. (2020). Role of erosion in creating thrust recesses in a critical-taper wedge: An example from Eastern Tibet. *Earth and Planetary Science Letters*, 540, 116270. <https://doi.org/10.1016/j.epsl.2020.116270>
- Ma, J., Wu, C., Cui, X., Izon, G., Saito, R., & Summons, R. E. (2019). Biomarkers reveal episodic marine incursions within the non-marine. 2019, T53A-08. Qaidam Basin.
- Mao, L., Yi, H., Ji, C., & Xia, G. (2014). Petrography and carbon-oxygen isotope characteristics of the Cenozoic Lacustrine carbonate rocks in Qaidam Basin. *Geological Science and Technology Information*, 33(1), 41–48.
- McQuarrie, N., Ehlers, T. A., Barnes, J. B., & Meade, B. (2008). Temporal variation in climate and tectonic coupling in the central Andes. *Geology*, 36(12), 999–1002. <https://doi.org/10.1130/g25124a.1>
- McRivette, M. W., Yin, A., Chen, X., & Gehrels, G. E. (2019). Cenozoic basin evolution of the central Tibetan plateau as constrained by U-Pb detrital zircon geochronology, sandstone petrology, and fission-track thermochronology. *Tectonophysics*, 751, 150–179. <https://doi.org/10.1016/j.tecto.2018.12.015>
- Meijer, N., Dupont-Nivet, G., Abels, H. A., Kaya, M. Y., Licht, A., Xiao, M., et al. (2019). Central Asian moisture modulated by proto-Paratethys Sea incursions since the early Eocene. *Earth and Planetary Science Letters*, 510, 73–84. <https://doi.org/10.1016/j.epsl.2018.12.031>
- Meyer, B., Tapponnier, P., Bourjot, L., Métivier, F., Gaudemer, Y., Peltzer, G., et al. (1998). Crustal thickening in Gansu-Qinghai, lithospheric mantle subduction, and oblique, strike-slip controlled growth of the Tibet plateau. *Geophysical Journal International*, 135(1), 1–47. <https://doi.org/10.1046/j.1365-246x.1998.00567.x>
- Molnar, P., England, P., & Martinod, J. (1993). Mantle dynamics, uplift of the Tibetan Plateau, and the Indian monsoon. *Reviews of Geophysics*, 31(4), 357–396. <https://doi.org/10.1029/93rg02030>
- Molnar, P., & Lyon-Caen, H. (1988). Some simple physical aspects of the support, structure, and evolution of mountain belts. In S. P. Clark Jr., B. C. Burchfiel, J. Suppe (Eds.), *Processes in continental lithospheric deformation*. p. 0. Geological Society of America.
- Mulch, A., & Chamberlain, C. P. (2006). The rise and growth of Tibet. *Nature*, 439(7077), 670–671. <https://doi.org/10.1038/439670a>
- Murphy, M. A., Yin, A., Harrison, T. M., Dürr, S. B., Z, C., Ryerson, F. J., et al. (1997). Did the Indo-Asian collision alone create the Tibetan plateau? *Geology*, 25(8), 719–722. [https://doi.org/10.1130/0091-7613\(1997\)025<0719:dtiaca>2.3.co;2](https://doi.org/10.1130/0091-7613(1997)025<0719:dtiaca>2.3.co;2)
- Nie, J., Ren, X., Saylor, J. E., Su, Q., Horton, B. K., Bush, M. A., et al. (2019). Magnetic polarity stratigraphy, provenance, and paleoclimate analysis of Cenozoic strata in the Qaidam Basin, NE Tibetan Plateau. *GSA Bulletin*, 132(1–2), 310–320. <https://doi.org/10.1130/b35175.1>
- Nie, J., Ruetenik, G., Gallagher, K., Hoke, G., Garzione, C. N., Wang, W., et al. (2018). Rapid incision of the Mekong River in the middle Miocene linked to monsoonal precipitation. *Nature Geoscience*, 11(12), 944. <https://doi.org/10.1038/s41561-018-0244-z>
- Poblete, F., Nivet, G. D., Licht, A., van Hinsbergen, D. J. J., Roperch, P., Mihalynuk, M. G., et al. (2021). Toward interactive global paleogeographic maps, new reconstructions at 60, 40 and 20 Ma. *Earth-Science Reviews*, 214, 103508. <https://doi.org/10.1016/j.earscirev.2021.103508>
- Porter, S. C. (2001). Chinese loess record of monsoon climate during the last glacial-interglacial cycle. *Earth-Science Reviews*, 54(1–3), 115–128. [https://doi.org/10.1016/s0012-8252\(01\)00043-5](https://doi.org/10.1016/s0012-8252(01)00043-5)
- Prell, W. L., & Kutzbach, J. E. (1992). Sensitivity of the Indian monsoon to forcing parameters and implications for its evolution. *Nature*, 360(6405), 647–652. <https://doi.org/10.1038/360647a0>
- Quade, J., Breecker, D. O., Daëron, M., & Eiler, J. (2011). The paleoaltimetry of Tibet: An isotopic perspective. *American Journal of Science*, 311(2), 77–115. <https://doi.org/10.2475/02.2011.01>

- Ren, X., Nie, J., Saylor, J. E., Wang, X., Liu, F., & Horton, B. K. (2020). Temperature control on silicate weathering intensity and evolution of the Neogene East Asian summer monsoon. *Geophysical Research Letters*, 47(15), e2020GL088808. <https://doi.org/10.1029/2020GL088808>
- Rieser, A. B., Bojar, A.-V., Neubauer, F., Genser, J., Liu, Y., Ge, X.-H., & Friedl, G. (2009). Monitoring Cenozoic climate evolution of northeastern Tibet: Stable isotope constraints from the western Qaidam Basin, China. *International Journal of Earth Sciences*, 98(5), 1063–1075. <https://doi.org/10.1007/s00531-008-0304-5>
- Robinson, D. M., Dupont-Nivet, G., Gehrels, G. E., & Zhang, Y. (2003). The Tula uplift, northwestern China: Evidence for regional tectonism of the northern Tibetan Plateau during late Mesozoic-early Cenozoic time. *Geological Society of America Bulletin*, 115(1), 35–47. [https://doi.org/10.1130/0016-7606\(2003\)115<0035:tunce>2.0.co;2](https://doi.org/10.1130/0016-7606(2003)115<0035:tunce>2.0.co;2)
- Rowley, D. B. (1996). Age of initiation of collision between India and Asia: A review of stratigraphic data. *Earth and Planetary Science Letters*, 145(1–4), 1–13. [https://doi.org/10.1016/s0012-821x\(96\)00201-4](https://doi.org/10.1016/s0012-821x(96)00201-4)
- Rowley, D. B., & Garzione, C. N. (2007). Stable Isotope-Based Paleoaltimetry. *Annual Review of Earth and Planetary Sciences*, 35(1), 463–508. <https://doi.org/10.1146/annurev.earth.35.031306.140155>
- Royden, L., & Karner, G. D. (1984). Flexure of the continental lithosphere beneath Apennine and Carpathian foredeep basins. *Nature*, 309(5964), 142–144. <https://doi.org/10.1038/309142a0>
- Saylor, J. E., Casturi, L., Shanahan, T. M., Nie, J., & Saadeh, C. M. (2016). Tectonic and climate controls on Neogene environmental change in the Zhada Basin, southwestern Tibetan Plateau. *Geology*, 44(11), 919–922. [G38173](https://doi.org/10.1130/G38173)
- Saylor, J. E., Jordan, J. C., Sundell, K. E., Wang, X., Wang, S., & Deng, T. (2018). Topographic growth of the Jishi Shan and its impact on basin and hydrology evolution, NE Tibetan Plateau. *Basin Research*, 30(3), 544–563. <https://doi.org/10.1111/bre.12264>
- Sclater, J. G., & Christie, P. A. F. (1980). Continental stretching: An explanation of the Post-Mid-Cretaceous subsidence of the central North Sea Basin. *Journal of Geophysical Research*, 85(B7), 3711–3739. <https://doi.org/10.1029/jb085ib07p03711>
- Song, B., Spicer, R. A., Zhang, K., Ji, J., Farnsworth, A., Hughes, A. C., et al. (2020). Qaidam Basin leaf fossils show northeastern Tibet was high, wet and cool in the early Oligocene. *Earth and Planetary Science Letters*, 537, 116175. <https://doi.org/10.1016/j.epsl.2020.116175>
- Spicer, R. A. (2017). Tibet, the Himalaya, Asian monsoons and biodiversity - In what ways are they related?. *Plant Diversity*, 39(5), 233–244. <https://doi.org/10.1016/j.pld.2017.09.001>
- Staisch, L. M., Niemi, N. A., Clark, M. K., & Chang, H. (2020). The Cenozoic evolution of crustal shortening and left-lateral shear in the Central East Kunlun Shan: Implications for the uplift history of the Tibetan Plateau. *Tectonics*, 39(9), e2020TC006065. <https://doi.org/10.1029/2020tc006065>
- Su, T., Spicer, R. A., Wu, F. X., Farnsworth, A., Huang, J., Rio, C. D., et al. (2020). A Middle Eocene lowland humid subtropical “Shangri-La” ecosystem in central Tibet. In *Proceedings of the national Academy of Sciences*. 2020012647
- Sun, D., Liu, D., Chen, M., An, Z., & John, S. (1997). Magnetostratigraphy and palaeoclimate of red clay sequences from Chinese Loess Plateau. *Science in China - Series D: Earth Sciences*, 40(4), 337–343. <https://doi.org/10.1007/bf02877564>
- Sun, X., & Wang, P. (2005). How old is the Asian monsoon system? Palaeobotanical records from China. *Palaeogeography, Palaeoclimatology, Palaeoecology*, 222(3), 181–222. <https://doi.org/10.1016/j.palaeo.2005.03.005>
- Sun, Y., Shaw, J. H., Guan, S., Ma, D., & Ma, X. (2020). Development and growth of basement-involved structural wedges in the northwestern Qaidam Basin, China. *Bulletin*, 104(5), 1091–1113. <https://doi.org/10.1306/11111918076>
- Tapponnier, P., Xu, Z. Q., Roger, F., Meyer, B., Arnaud, N., Wittlinger, G., & Yang, J. S. (2001). Oblique stepwise rise and growth of the Tibet Plateau. *Science*, 294(5547), 1671–1677. <https://doi.org/10.1126/science.105978>
- Turcotte, D., and G. Schubert, (2002), *Geodynamics*, 456. pp. edited, Cambridge Univ. Press.
- Wang, C., Zhao, X., Liu, Z., Lippert, P. C., Graham, S. A., Coe, R. S., et al. (2008). Constraints on the early uplift history of the Tibetan Plateau. *Proceedings of the National Academy of Sciences of the United States of America*, 105(13), 4987–4992. <https://doi.org/10.1073/pnas.0703595105>
- Wang, E., Kamp, P. J. J., Xu, G., Hodges, K. V., Meng, K., Chen, L., et al. (2015). Flexural bending of southern Tibet in a retro foreland setting. *Scientific Reports*, 5(1), 12076. <https://doi.org/10.1038/srep12076>
- Wangen, M. (2010). *Physical principles of sedimentary basin analysis*. Cambridge University Press.
- Wang, F., Shi, W., Zhang, W., Wu, L., Yang, L., Wang, Y., & Zhu, R. (2017). Differential growth of the northern Tibetan margin: Evidence for oblique stepwise rise of the Tibetan Plateau. *Scientific Reports*, 7, 41164. <https://doi.org/10.1038/srep41164>
- Wang, L., MacLennan, S. A., & Cheng, F. (2020). From a proximal-deposition-dominated basin sink to a significant sediment source to the Chinese Loess Plateau: Insight from the quantitative provenance analysis on the Cenozoic sediments in the Qaidam basin, northern Tibetan Plateau. *Palaeogeography, Palaeoclimatology, Palaeoecology*, 556, 109883. <https://doi.org/10.1016/j.palaeo.2020.109883>
- Wang, M., & Shen, Z.-K. (2020). Present-day crustal deformation of continental China derived from GPS and its tectonic implications. *Journal of Geophysical Research: Solid Earth*, 125(2), e2019JB018774. <https://doi.org/10.1029/2019jb018774>
- Wang, P., Clemens, S., Beaufort, L., Braconnot, P., Ganssen, G., Jian, Z., et al. (2005). Evolution and variability of the Asian monsoon system: State of the art and outstanding issues. *Quaternary Science Reviews*, 24(5), 595–629. <https://doi.org/10.1016/j.quascirev.2004.10.002>
- Wang, W., Zheng, W., Zhang, P., Li, Q., Kirby, E., Yuan, D., et al. (2017). Expansion of the Tibetan Plateau during the Neogene. *Nature Communications*, 8, 15887. <https://doi.org/10.1038/ncomms15887>
- Wang, X., Qiu, Z., Li, Q., Wang, B., Downs, W. R., Xie, G., et al. (2007). Vertebrate paleontology, biostratigraphy, geochronology, and paleoenvironment of Qaidam Basin in northern Tibetan Plateau. *Palaeogeography, Palaeoclimatology, Palaeoecology*, 254(3–4), 363–385. <https://doi.org/10.1016/j.palaeo.2007.06.007>
- Wei, Y., Xiao, A., Wu, L., Mao, L., Zhao, H., Shen, Y., & Wang, L. (2016). Temporal and spatial patterns of Cenozoic deformation across the Qaidam Basin, Northern Tibetan Plateau. *Terra Nova*, 28(6), 409–418. <https://doi.org/10.1111/ter.12234>
- West, A., Galy, A., & Bickle, M. (2005). Tectonic and climatic controls on silicate weathering. *Earth and Planetary Science Letters*, 235(1), 211–228. <https://doi.org/10.1016/j.epsl.2005.03.020>
- Wu, C., Yin, A., Zuza, A. V., Zhang, J., Liu, W., & Ding, L. (2016). Pre-Cenozoic geologic history of the central and northern Tibetan Plateau and the role of Wilson cycles in constructing the Tethyan orogenic system. *Lithosphere*, 8(3), 254–292. <https://doi.org/10.1130/l1494.1>
- Wu, C., Zuza, A. V., Chen, X., Ding, L., Levy, D. A., Liu, C., et al. (2019a). Tectonics of the Eastern Kunlun Range: Cenozoic reactivation of a Paleozoic-Early Mesozoic orogen. *Tectonics*, 38(5), 1609–1650. <https://doi.org/10.1029/2018tc005370>
- Wu, C., Zuza, A. V., Zhou, Z., Yin, A., McRivette, M. W., Chen, X., et al. (2019b). Mesozoic-Cenozoic evolution of the Eastern Kunlun Range, central Tibet, and implications for basin evolution during the Indo-Asian collision. *Lithosphere*, 11(4), 524–550. <https://doi.org/10.1130/l1065.1>
- Wu, L., Lin, X., Cowgill, E., Xiao, A., Cheng, X., Chen, H., et al. (2019). Middle Miocene reorganization of the Altyn Tagh fault system, northern Tibetan Plateau. *GSA Bulletin*, 131(7–8), 1157–1178. <https://doi.org/10.1130/b31875.1>

- Wu, L., Xiao, A., Ma, D., Li, H., Xu, B., Shen, Y., & Mao, L. (2014). Cenozoic fault systems in southwest Qaidam Basin, northeastern Tibetan Plateau: Geometry, temporal development, and significance for hydrocarbon accumulation. *Bulletin*, 98(6), 1213–1234. <https://doi.org/10.1306/11131313087>
- Xia, W. C., Zhang, N., Yuan, X. P., Fan, L. S., & Zhang, B. S. (2001). Cenozoic Qaidam basin, China: A stronger tectonic inverted, extensional rifted basin. *American Association of Petroleum Geologists Bulletin*, 85(4), 715–736.
- Xie, Y., Wu, F., & Fang, X. (2019). Middle Eocene East Asian monsoon prevalence over southern China: Evidence from palynological records. *Global and Planetary Change*, 175, 13–26. <https://doi.org/10.1016/j.gloplacha.2019.01.019>
- Yang, F., Ma, Z. Q., Xu, T. C., & Ye, S. J. (1992). A Tertiary paleomagnetic stratigraphic profile in Qaidam basin (in Chinese with English abstract). *Acta Petrolei Sinica*, 13(2), 97–101.
- Yang, Y., & Liu, M. (2002). Cenozoic deformation of the Tarim plate and the implications for mountain building in the Tibetan Plateau and the Tian Shan. *Tectonics*, 21(6), 9-1-9-17. <https://doi.org/10.1029/2001tc001300>
- Yin, A., Dang, Y. Q., Wang, L. C., Jiang, W. M., Zhou, S. P., Chen, X. H., et al. (2008a). Cenozoic tectonic evolution of Qaidam basin and its surrounding regions (Part 1): The southern Qilian Shan-Nan Shan thrust belt and northern Qaidam basin. *Geological Society of America Bulletin*, 120(7–8), 813–846. <https://doi.org/10.1130/b26180.1>
- Yin, A., Dang, Y. Q., Zhang, M., Chen, X. H., & McRivette, M. W. (2008b). Cenozoic tectonic evolution of the Qaidam basin and its surrounding regions (Part 3): Structural geology, sedimentation, and regional tectonic reconstruction. *Geological Society of America Bulletin*, 120(7–8), 847–876. <https://doi.org/10.1130/b26232.1>
- Yin, A., Dang, Y., Zhang, M., McRivette, M. W., Burgess, W. P., & Chen, X. (2007). Cenozoic tectonic evolution of Qaidam basin and its surrounding regions (part 2): Wedge tectonics in southern Qaidam basin and the Eastern Kunlun Range. *Geological Society of America Special Paper*, 433, 369–390. [https://doi.org/10.1130/2007.2433\(18\)](https://doi.org/10.1130/2007.2433(18))
- Yin, A., & Harrison, T. M. (2000). Geologic evolution of the Himalayan-Tibetan orogen. *Annual Review of Earth and Planetary Sciences*, 28(1), 211–280. <https://doi.org/10.1146/annurev.earth.28.1.211>
- Yuan, D. Y., Ge, W. P., Chen, Z. W., Li, C. Y., Wang, Z. C., Zhang, H. P., et al. (2013). The growth of northeastern Tibet and its relevance to large-scale continental geodynamics: A review of recent studies. *Tectonics*, 32(5), 1358–1370. <https://doi.org/10.1002/tect.20081>
- Zhang, C., Cheng, F., Huang, G., Huang, Y., Xing, C., Guan, B., et al. (2013). Sediment and reservoir characteristics with reservoir evaluation of the Lulehe Formation in Qie 16 block of Kunbei oilfield in Qaidam Basin. *Acta Petrologica Sinica*, 29(8), 2883–2894.
- Zhang, R., Zhang, Z., & Jiang, D. (2018). Global cooling contributed to the establishment of a modern-like East Asian monsoon climate by the Early Miocene. *Geophysical Research Letters*, 45(21), 11941–11948. <https://doi.org/10.1029/2018gl079930>
- Zhang, W. (2007). High-resolution megnetostratigraphy of the Cenozoic Qaidam Basin, implications for the uplift of Tibetan Plateau. In *Chinese with English abstract*. LanZhou University.
- Zhao, J., Jin, Z., Mooney, W. D., Okaya, N., Wang, S., Gao, X., et al. (2013). Crustal structure of the central Qaidam basin imaged by seismic wide-angle reflection/refraction profiling. *Tectonophysics*, 584, 174–190. <https://doi.org/10.1016/j.tecto.2012.09.005>
- Zheng, D., Wang, W., Wan, J., Yuan, D., Liu, C., Zheng, W., et al. (2017). Progressive northward growth of the northern Qilian Shan-Hexi Corridor (northeastern Tibet) during the Cenozoic. *Lithosphere*, 9(3), 408–416. <https://doi.org/10.1130/l1587.1>
- Zuza, A., Wu, C., Reith, R., Yin, A., Li, J., Zhang, J., et al. (2018a). Tectonic evolution of the Qilian Shan: An early Paleozoic orogen reactivated in the Cenozoic. *Geological Society of America Bulletin*, 130(5–6), 881–925. <https://doi.org/10.1130/b31721.1>
- Zuza, A. V., Cheng, X., & Yin, A. (2016). Testing models of Tibetan Plateau formation with Cenozoic shortening estimates across the Qilian Shan-Nan Shan thrust belt. *Geosphere*, 12(2), 501–532. <https://doi.org/10.1130/ges01254.1>
- Zuza, A. V., Wu, C., Wang, Z., Levy, D. A., Li, B., Xiong, X., & Chen, X. (2018b). Underthrusting and duplexing beneath the northern Tibetan Plateau and the evolution of the Himalayan-Tibetan orogen. *Lithosphere*, 11(2), 209–231. <https://doi.org/10.1130/l1042.1>